

Prediction of surface admittance impulse responses from frequency-dependent sound absorption coefficients

Csaba Huszty¹

ENTEL Engineering Research & Consulting Ltd. Inspired Acoustics division
Szépvölgyi út 32., H-1025 Budapest, Hungary

Gergely Firtha^{2,3}

Department of Networked Systems and Services, Faculty of Electric Engineering, Budapest University of Technology and Economics, Műegyetem rkp. 3., H-1111 Budapest, Hungary
ENTEL Engineering Research & Consulting Ltd. Inspired Acoustics division
Szépvölgyi út 32., H-1025 Budapest, Hungary;

ABSTRACT

In numerical room acoustic modeling certain material properties are required as inputs for setting the boundary conditions for the calculations. In finite element or finite difference models, locally reactive boundaries are often represented as FIR or IIR filters. However, most building material manufacturers provide sound absorption coefficient or equivalent absorption area data only, in accordance with the relevant standards, so a method to convert sound absorption to admittance or impedance impulse responses is required. Since there is a loss of information when admittance is converted to sound absorption coefficients, the conversion in the opposite direction has multiple solutions. We derive an iterative method of determining either the impedance or admittance impulse response from arbitrary, frequency-dependent diffuse sound absorption coefficients and validate it with the transfer matrix method. We present the implementation of the method in the soundy.ai application.

1. INTRODUCTION

The diffuse absorption coefficient is a well-established parameter used to describe acoustic materials in the context of room acoustic control. It can be easily measured in a reverberation chamber by estimating the decrease in reverberation time, as specified in ISO 354:2003 [1]. Additionally, diffuse absorption can be incorporated as a simple wall material property in statistical-based room acoustics simulation software.

However, numerical methods that aim to solve the wave equation in enclosures, such as finite element and finite difference methods, require appropriate boundary conditions for the absorbing boundary surfaces. As a simplification, boundaries are often approximated as locally reactive, disregarding wave propagation within the bounding surface [2]. Locally reactive surfaces can be described using impedance or admittance boundary conditions, which couple the surface pressure and velocity at the point of interest. Nevertheless, even for locally reactive surfaces, the angle-dependent absorption coefficient (which inherently lacks phase information of the surface

¹huszty.csaba@entel.hu

²firtha@hit.bme.hu

³gergely.firtha@entel.hu

impedance/admittance) neglects the phase information and integrates absorption from all possible angles. Consequently, acquiring impedance/admittance properties solely from diffuse absorption characteristics presents a highly underdetermined problem, leading to an infinite number of solutions even with locally reactive assumptions.

Several studies have attempted impedance reconstruction from absorption functions by assuming an underlying physical model and employing parameter fitting or considering random incidence absorption [3–5]. However, in the context of numerical room acoustics simulations, an impedance/admittance function that achieves the desired diffuse absorption characteristics may suffice.

This paper presents a numerical algorithm that enables the estimation of impedance/admittance from diffuse absorption characteristics, assuming locally reactive boundaries. The method is based on the causality condition prescribed for the bounding surfaces, which is a physically motivated requirement. By incorporating causality through the Discrete Hilbert Transform, the problem can be formulated as a system of nonlinear equations that can be solved using the Newton-Raphson method. Since the problem still has an infinite number of solutions, optimizing for impedance or admittance functions yields different results.

The validity of the numerical method is demonstrated by examining simple absorber structures, including a single layer of porous absorber and a simple plate absorber. The results show that the proposed approach can yield both suitable impedance and admittance functions, ensuring the desired diffuse absorption characteristics. However, when matching the absorption to an underlying physical model, deriving the admittance function is a viable alternative to evaluating the surface impedance.

2. PROBLEM FORMULATION

Let's assume an infinite, locally reactive surface. The impedance at each point of the surface is given by $Z_{\text{surf}}(\omega) = \frac{P(\omega)}{V(\omega)}$, or alternatively the surface admittance $A_{\text{surf}}(\omega) = 1/Z_{\text{surf}}(\omega)$. To simplify the subsequent discussion, we introduce the normalized surface impedance and admittance as $Z_A(\omega) = Z_{\text{surf}}(\omega)/Z_0$, and $A_A(\omega) = A_{\text{surf}}(\omega) \cdot Z_0$ respectively. The directional absorption coefficient is obtained from the normalized surface impedance and admittance as

$$\alpha(\omega, \theta) = 1 - |R(\omega, \theta)|^2 = \frac{4\text{Re}(Z_A)/\cos\theta}{|Z_A + 1/\cos\theta|^2} = \frac{4\text{Re}(A_A)\cos\theta}{|A_A + \cos\theta|^2}. \quad (1)$$

where $R(\omega, \theta)$ is the reflection coefficient. From the directional absorption coefficient the diffuse field absorption coefficient for random incidence is defined by integrating over the angle of incidence, calculated as

$$\alpha_d(\omega) = \frac{\int_0^{\theta_f} \alpha(\omega, \theta) \sin\theta \cos\theta d\theta}{\int_0^{\theta_f} \sin\theta \cos\theta d\theta}. \quad (2)$$

where θ_f is the final angle value of the integration range, for the sake of simplicity chose to be $\theta_f = \frac{\pi}{2}$. With this limit of integration $\int_0^{\pi/2} \sin\theta \cos\theta d\theta = 0.5$, and the diffuse absorption field coefficient reads as

$$\alpha_d(\omega) = 8 \int_0^{\pi/2} \frac{\text{Re}(Z_A(\omega))}{|Z_A(\omega) + 1/\cos\theta|^2} \sin\theta d\theta = 8 \int_0^{\pi/2} \frac{\text{Re}(A_A(\omega))}{|A_A(\omega) + \cos\theta|^2} \cos^2\theta \sin\theta d\theta. \quad (3)$$

In the following our aim is to express the surface impedance Z_A and surface admittance A_A assuming that the diffuse absorption coefficient, $\alpha_d(\omega)$ is given. The main goal of the derivation is to retrieve phase information merely from the real value or the absolute value of the impedance/admittance function. In order to arrive at a solution for the underdetermined problem the following physically-based assumptions are made (presented for the impedance, however, the following criteria equivalently holds without change for the admittance $A_A(\omega)$):

- *Causality*: As in the time domain the impedance function describes the pressure response for a point like velocity excitation over the surface, the response signal should not precede the excitation, i.e. the temporal representation of the impedance function has to be causal. In the temporal domain this yields

$$Z_A(t) = 0, \quad \text{for } t < 0. \quad (4)$$

In the frequency domain this is equivalent to the statement that $Z_A(\omega)$ is analytical, i.e. the imaginary part of the complex valued impedance function is the Hilbert transform of the real part [5, 6]

$$Z_A(\omega) = r(\omega) - j\mathcal{H}(r(\omega)) = r(\omega) - \frac{j}{\pi} \int_{-\infty}^{\infty} \frac{r(y)}{\omega - y} dy, \quad (5)$$

where $r(\omega) = \text{Re}(Z_A(\omega))$ and $\mathcal{H}()$ denotes the Hilbert transform [7].

- *Passivity*: The boundary should not generate energy additionally to the sound field. Mathematically this requirement can be formulated as

$$\text{Re}(Z_A(\omega)) \geq 1, \quad \text{for } \omega \in \mathbb{R} \quad (6)$$

- *Real valued time domain description*: Since describing a physical process, the casual temporal representation of the impedance is real valued. In the frequency domain this means

$$Z_A^*(\omega) = Z_A(-\omega). \quad (7)$$

This latter requirement can be automatically satisfied by evaluating the following numerical method up to the half of the sampling frequency, and afterwards symmetrizing the spectrum.

With taking the causality condition into consideration the diffuse absorption coefficient Equation 3 can be written analytically as

$$\begin{aligned} \alpha_d(\omega) &= 8 \int_0^{\pi/2} \frac{r(\omega)}{|r(\omega) - j\mathcal{H}(r(\omega)) + 1/\cos\theta|^2} \sin\theta d\theta = \\ &= 8 \int_0^{\pi/2} \frac{r(\omega)}{(r(\omega) + 1/\cos\theta)^2 + \mathcal{H}(r(\omega))^2} \sin\theta d\theta. \end{aligned} \quad (8)$$

Similarly, with expressing the absorption coefficient in terms of the admittance, denoting $A_A(\omega) = x(\omega) + jy(\omega)$

$$\alpha_d(\omega) = 8 \int_0^{\pi/2} \frac{x(\omega)}{(x(\omega) + \cos\theta)^2 + \mathcal{H}(x(\omega))^2} \cos^2\theta \sin\theta d\theta. \quad (9)$$

is yielded.

3. NUMERICAL METHOD FOR EVALUATING THE IMPEDANCE/ADMITTANCE

In the previous section it was shown how the diffuse absorption coefficient can be expressed merely in terms of the real part of the surface impedance or the admittance. Now a numerical method is discussed in order to solve Equation 8 or Equation 9 for either the real part of the impedance or admittance, first discussed for the impedance case.

3.1. Discretization of the involved equations

In order to solve the Equation 8 for $r(\omega)$ all the involved quantities are discretized with a simple sampling discretization scheme.

In the derivation the following nomenclature is used:

- $\alpha = \alpha_n$ and $\mathbf{r} = r_n$ are the elements of the frequency dependent target absorption coefficient vector and the real part of the impedance to be evaluated, respectively. Both are discretized into N elements from ω_0 to πf_s .
- $\theta = \theta_i$ denotes the elements of the incidence angle-vector with I elements, spanning from 0 to $\pi/2$.
- According to [8] it is possible to realize the discrete Hilbert transform (DHT) in a matrix form, by multiplying the input vector with the Hilbert matrix. The elements of the $N \times N$ -sized Hilbert matrix $\mathbf{H} = H_{nm}$ are given as

$$\mathbf{H} = \frac{1}{N} \begin{bmatrix} 0 & -c_1 & 0 & -c_3 & \dots & -c_{N-1} \\ c_1 & 0 & -c_1 & 0 & \dots & 0 \\ 0 & c_1 & 0 & -c_1 & \dots & -c_{N-3} \\ \cdot & \cdot & \cdot & \cdot & \dots & \cdot \\ \cdot & \cdot & \cdot & \cdot & \dots & \cdot \\ c_{N-1} & 0 & c_{N-3} & 0 & \dots & 0 \end{bmatrix}. \quad (10)$$

With this notation Equation 8 is discretized to

$$\alpha_n = 8 \frac{\pi}{2(I-1)} \sum_{i=0}^{I-1} \frac{r_n \sin \theta_i}{(r_n + 1/\cos \theta_i)^2 + \left(\sum_{m=0}^{N-1} H_{nm} r_m \right)^2} \quad (11)$$

resulting in the system of N number of non-linear equations coupled by the Hilbert matrix, which has to be solved for each r_n simultaneously.

3.2. Iterative solution for the non-linear system of equations

The system of non-linear equations can be solved by the Newton-Raphson method iteratively. Starting out from an initial impedance vector \mathbf{r}^0 , in the $j+1$ -th iteration the solution vector, yielding the roots of expression $F(\mathbf{r}^j)$ is obtained as

$$\mathbf{r}^{j+1} = \mathbf{r}^j - \mathbf{J}_F(\mathbf{r}^j)^{-1} F(\mathbf{r}^j). \quad (12)$$

The iteration is performed until convergence is achieved, i.e. while $|\mathbf{r}^{j+1} - \mathbf{r}^j| = |\mathbf{J}_F(\mathbf{r}^j)^{-1} F(\mathbf{r}^j)| < \epsilon$.

In the problem under consideration the expression to be minimized is given by

$$F(\mathbf{r}) = \alpha_n - 8 \frac{\pi}{2(I-1)} \sum_{i=0}^{I-1} \frac{r_n \sin \theta_i}{(r_n + 1/\cos \theta_i)^2 + \left(\sum_{m=0}^{N-1} H_{nm} r_m \right)^2} \quad (13)$$

and the $N \times N$ -sized Jacobian matrix is obtained from the partial derivative as

$$\mathbf{J}_F(\mathbf{r}) = J_{nk} = \frac{\partial}{\partial r_k} F(\mathbf{r}) = -8 \frac{\pi}{2(I-1)} \sum_{i=0}^{I-1} \frac{\partial}{\partial r_k} \frac{r_n \sin \theta_i}{(r_n + 1/\cos \theta_i)^2 + \left(\sum_{m=0}^{N-1} H_{nm} r_m \right)^2}. \quad (14)$$

Performing the required differentiation the Jacobian reads as

$$J_{nk} = -8 \frac{\pi}{2(I-1)} \sum_{i=0}^{I-1} \frac{I_{nk} \left((r_n + 1/\cos \theta_i)^2 + \left(\sum_{m=0}^{N-1} H_{nm} r_m \right)^2 \right) - r_n \left(2r_n I_{nk} + 2 \frac{I_{nk}}{\cos \theta_i} + 2 \left(\sum_{m=0}^{N-1} H_{nm} r_m \right) H_{nk} \right)}{\left((r_n + 1/\cos \theta_i)^2 + \left(\sum_{m=0}^{N-1} H_{nm} r_m \right)^2 \right)^2} \sin \theta_i. \quad (15)$$

With the above iteration the real part of the impedance function can be obtained. Finally, the complex impedance can be calculated as

$$\mathbf{Z}_A = \mathbf{r} - \mathbf{jHr}. \quad (16)$$

3.3. Optimal choice of the initial vector

It is important point out that due to the lack of the phase information in the absorption coefficient, therefore, an infinite number of complex, casual impedance functions result in the same absorption, and Equation 8 is satisfied by infinite number of $r(\omega)$ functions. Therefore, the choice of the initial vector in the numerical iteration is crucial for both convergence and the properties of the obtained solution.

A suitable choice for the initial vector is $\mathbf{r}^0 = 0$. With this choice the initial Jacobian J_{nk}^0 and the expression to be minimized $F^0(\mathbf{r})$ reads as

$$J_{nk}^0 = \mathbf{J}_F^0 = -8 I_{nk} \underbrace{\sum_{i=0}^{I-1} \cos^2 \theta_i \sin \theta_i \frac{\pi}{2(I-1)}}_{\approx 1/3} \approx -\frac{8}{3} \mathbf{I} \quad \rightarrow \quad (\mathbf{J}_F^0)^{-1} = -\frac{3}{8} \mathbf{I} \quad (17)$$

$$F^0(\mathbf{r}) = \alpha_n. \quad (18)$$

As a result, at the first iteration the correction vector is given by

$$-(\mathbf{J}_F^0)^{-1} F^0(\mathbf{r}) = \frac{3}{8} \alpha. \quad (19)$$

This leads to convergence towards positive solution vectors, inherently ensuring the passivity condition. Moreover, with this choice, the iteration is likely to converge to the solution for which $|\mathbf{r}|$ is minimal, resulting in the "minimal phase" solution of the problem. Physically, the minimal phase impedance implies that the considered material reradiates energy to the fluid earlier than any other non-minimum phase material, which is advantageous for including the material in time-domain numerical simulations [9, 10]. However, a rigorous mathematical proof that the solution with minimal $|\mathbf{r}|$ is indeed a minimal phase solution is the subject of further investigation.

3.4. The iterative scheme for obtaining the surface admittance

Assuming that the iteration scheme aims to directly solve for the surface admittance in the discretization scheme, the iteration steps and considerations regarding the initial vector remain identical to those presented in the previous subsection. The iteration needs to be solved for the real part of the admittance function, denoted as $\mathbf{x} = x_n$. In this case the expression to be minimized is given by

$$F(\mathbf{r}) = \alpha_n - 8 \frac{\pi}{2(I-1)} \sum_{i=0}^{I-1} \frac{x_n \cos^2 \theta_i \sin \theta_i}{(x_n + \cos \theta_i)^2 + \left(\sum_{m=0}^{N-1} H_{nm} x_m \right)^2} \quad (20)$$

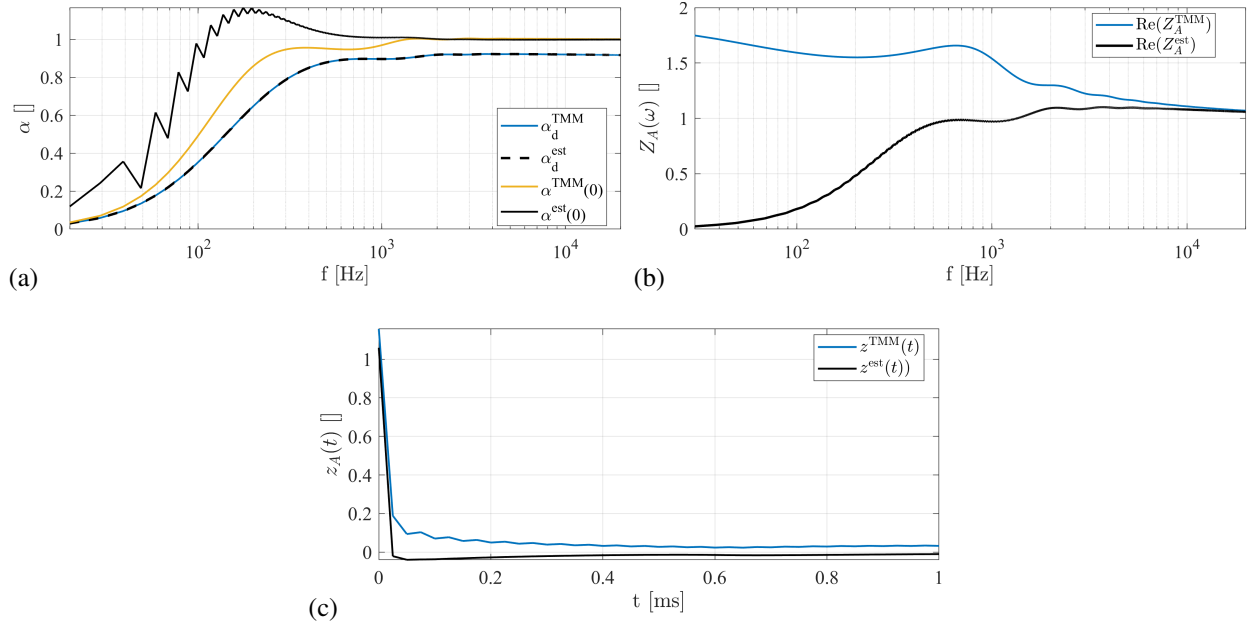


Figure 1: Result of calculating the surface impedance from the diffuse absorption coefficient in case of a porous absorber layer, depicting the diffuse and the normal absorption coefficient (a) the real part of impedance (b) and the time domain representation of the impedance function (c)

with the Jacobian given as

$$J_{nk} = -8 \frac{\pi}{2(I-1)}$$

$$\sum_{i=0}^{I-1} \frac{I_{nk} \left((x_n + \cos \theta_i)^2 + \left(\sum_{m=0}^{N-1} H_{nm} x_m \right)^2 \right) - x_n \left(2x_n I_{nk} + 2I_{nk} \cos \theta_i + 2 \left(\sum_{m=0}^{N-1} H_{nm} x_m \right) H_{nk} \right)}{\left((x_n + \cos \theta_i)^2 + \left(\sum_{m=0}^{N-1} H_{nm} x_m \right)^2 \right)^2} \cos^2 \theta_i \sin \theta_i. \quad (21)$$

By iterating from the initial vector $\mathbf{x}^0 = 0$ the real part of the admittance function can be obtained and the normalized admittance is given as

$$\mathbf{A}_A = \mathbf{x} - \mathbf{jHx}. \quad (22)$$

4. PERFORMANCE ANALYSIS OF THE PRESENTED METHOD

To validate the iteration scheme, the surface impedance and the resulting diffuse absorption coefficient were evaluated for layered locally reactive absorber structures using the 1D transfer matrix method (TMM) [11]. The advantage of employing an analytical model was the availability of the surface impedance in analytical form, facilitating a direct comparison with the numerically predicted impedance function.

The validation process encompassed two examples: a single layer of porous absorber and a plate absorber comprising a thin top plate, a layer of porous absorber, an air gap, and a rigid termination.

4.1. Results for a single porous layer

First, the obtained impedance and admittance functions were investigated for a porous layer with a thickness of $d = 10$ cm and a flow resistivity of $\sigma = 20,000$ Rayl/m, which represents the typical flow resistivity of a dense rockwool layer. The porous layer was modeled within the TMM framework as an equivalent fluid using the Miki model [12]. The surface impedance of the porous

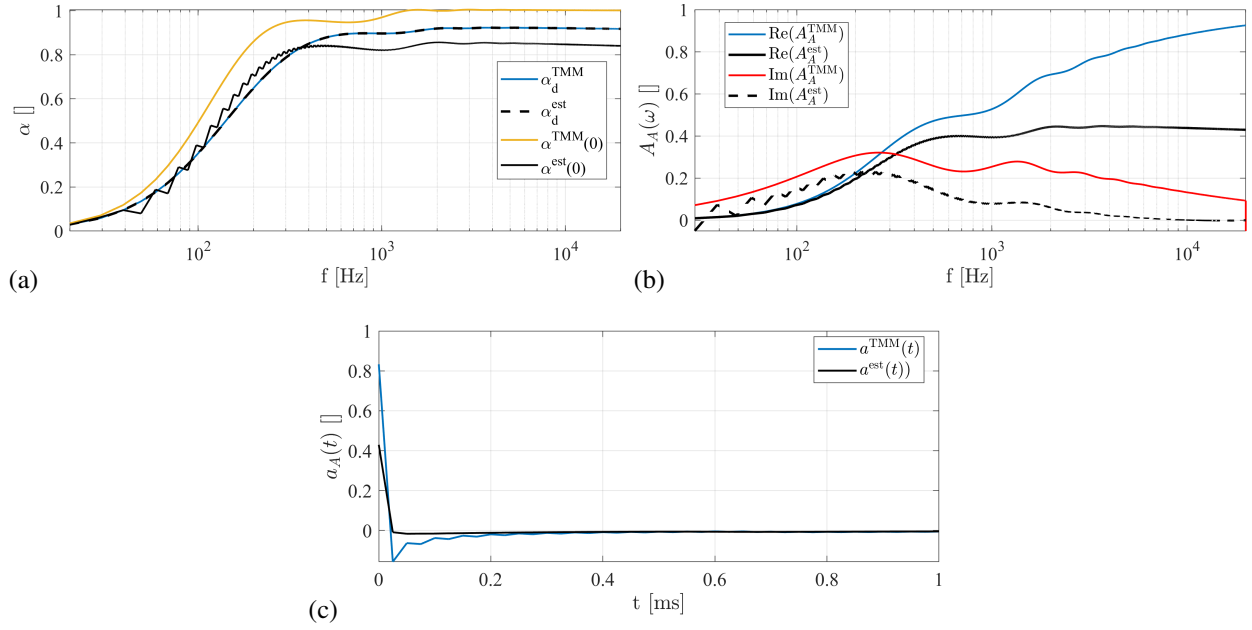


Figure 2: Result of calculating the surface admittance from the diffuse absorption coefficient in case of a porous absorber layer, depicting the diffuse and the normal absorption coefficient (a) the real part of admittance (b) and the time domain representation of the admittance function (c)

layer, terminated by a rigid backing, was calculated using the transfer matrix method. The diffuse absorption coefficient of the absorber was then computed from the surface impedance according to Equation 3. This diffuse absorption coefficient served as the input for the iterative method presented in the previous section to estimate the original surface impedance and admittance.

For both impedance and admittance estimation, the absorption function (as well as the impedance and admittance functions) was sampled at $N = 4096$ points with a sampling frequency of 40 kHz. The angular domain was sampled at $I = 16$ points from 0 to $\frac{\pi}{2}$, resulting in $d\theta = 6^\circ$. The initial vector $\mathbf{r}^0 = \mathbf{x}^0 = 0$ was chosen for the iterative algorithm in accordance with the considerations outlined in the previous section. A convergence threshold of $\epsilon = 10^{-10}$ was selected, leading to 17 iterations.

The results of the impedance estimation are shown in Figure 1. Figure (a) displays the input diffuse absorption coefficient α_{dTMM} along with the absorption function calculated from the iteratively estimated impedance function denoted as α_{dest} . A perfect match between the two is observed, indicating successful convergence to a valid solution vector. However, when examining the directional absorption coefficient for normal incidence, given by

$$\alpha(\omega, 0) = \frac{4\text{Re}(Z_A)}{|Z_A + 1|^2} = \frac{4\text{Re}(A_A)}{|A_A + 1|^2}, \quad (23)$$

significant discrepancies arise compared to the reference absorption. This error suggests that although the estimated impedance vector yields the same diffuse, weighted average absorption, it does not accurately estimate the underlying physical model. This is further confirmed in Figure (b), which illustrates the estimated real part of the impedance vector \mathbf{r} alongside the reference vector obtained analytically from the transfer matrix method. The figure indicates that the iterative method converged to a solution vector with minimal energy, but with notable deviations from the impedance of the actual 1D physical model. As a consequence, the temporal representation of the estimated impedance function also differs from the system's impedance impulse response, as depicted in Figure (c), which is calculated as the inverse Fourier transform of the estimated and reference impedances. Notably, the estimated impulse response concentrates the total energy of the response closer to the origin, suggesting that the numerical iteration converged towards a minimal-phase solution.

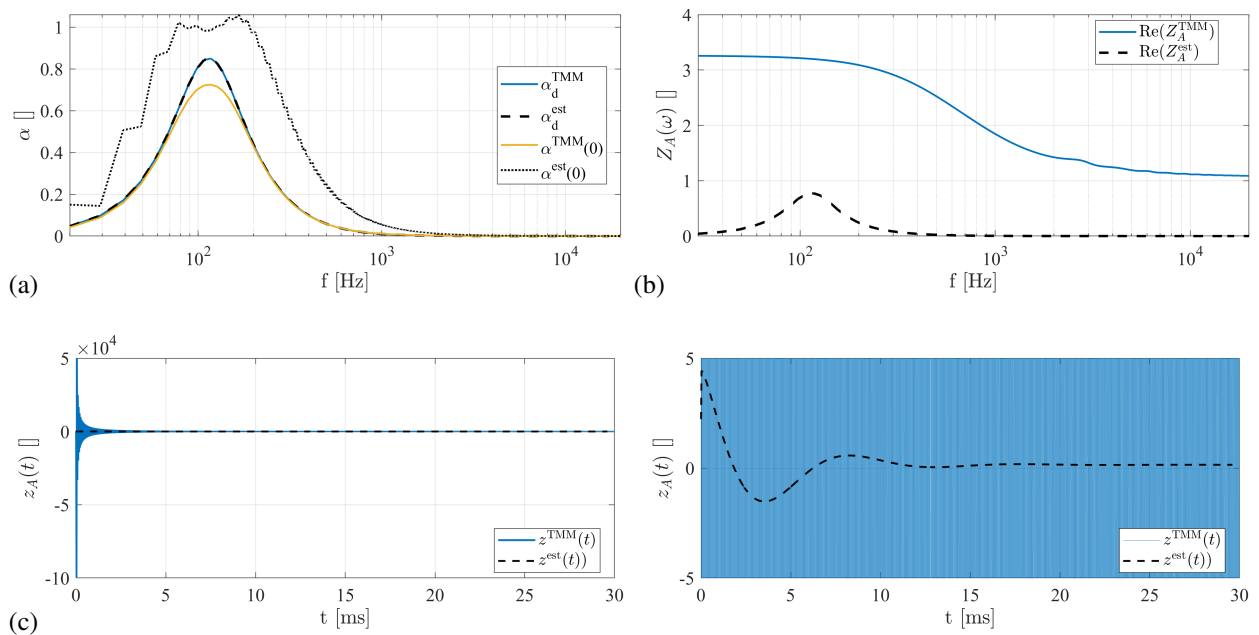


Figure 3: Result of calculating the surface impedance from the diffuse absorption coefficient in case of a plate resonator, depicting the diffuse and the normal absorption coefficient (a) the real part of impedance (b) and the time domain representation of the impedance function with different xy -scales (c)

The results of the iterative method for admittance estimation are shown in Figure 2. Once again, Figure (a) displays the diffuse and normal absorption coefficients calculated from the analytical and estimated admittance, Figure (b) shows the estimated real admittance vector, and Figure (c) illustrates the admittance response of the reference and estimated systems. Similar to the impedance case, the diffuse absorption coefficient calculated from the admittance estimation perfectly coincides with the reference, indicating that the iteration converged to a correct solution. However, the estimated admittance differs from the actual system's admittance. Nevertheless, in this case, the estimated admittance function, the directional absorption coefficient, and the admittance response approximate the reference vectors qualitatively better than in the impedance case. This observation suggests that the admittance solution provides a better approximation of the underlying physical model compared to the impedance solution.

4.2. Results for a plate absorber

Finally, the impedance/admittance estimation of a resonant absorber structure was conducted to investigate the case when the target absorption function exhibits a strong peak at a specific frequency.

The top limp membrane layer has a thickness of $h = 4$ mm and a density of 700 kg/m^3 , representing a typical firwood top plate. The porous layer at the back of the top plate has a thickness of $d = 5$ cm with a flow resistivity of $50,000 \text{ Rayl/m}$, representing dense mineral wool. Once again, the porous layer is modeled in the TMM framework using the Allard-Champoux model [13]. Finally, the porous layer is backed by an air gap of 5 cm and terminated by a rigid backing.

The results of the estimation are depicted for the impedance in Figure 3 and the admittance in Figure 4. Similarly to the simple porous absorber case, a perfect match is achieved between the estimated impedance and admittance and the target diffuse absorption coefficient. However, in the present example, the analytical and estimated real impedance differ significantly from the analytical reference (see Figure 3 (b)). This indicates that the estimated impedance provides a minimal energy solution for the target absorption, resulting in significant differences in the normal incidence

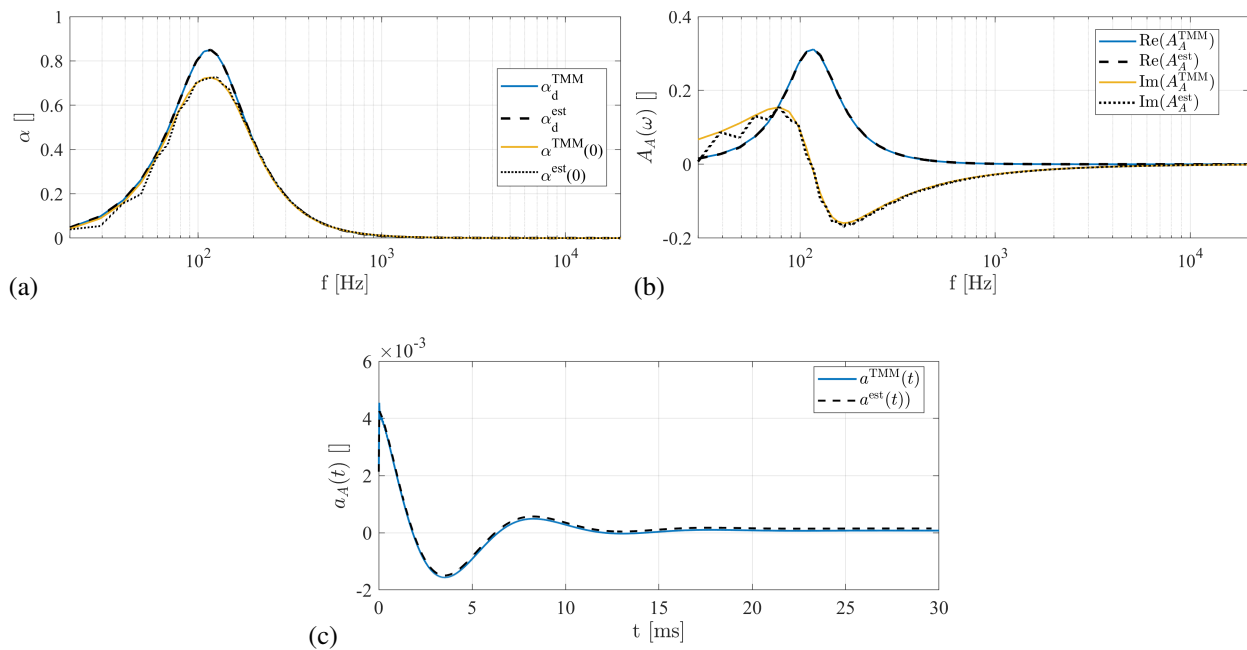


Figure 4: Result of calculating the surface admittance from the diffuse absorption coefficient in case of a plate resonator, depicting the diffuse and the normal absorption coefficient (a) the real part of admittance (b) and the time domain representation of the admittance function (c)

absorption (Figure 3 (b)) and the temporal impedance response (Figure 3 (c)).

On the other hand, in the present example, the estimated admittance function perfectly matches the analytical reference for both the real and imaginary parts (see Figure 4 (b)). As a result, the normal incidence absorption (Figure 3 (a)) and the temporal admittance response (Figure 4 (c)) also coincide. This coincidence can be explained by the fact that the analytical system is minimal-phase regarding its admittance. However, further research is needed to investigate the aspect of when the numerical iteration converges to the actual physical solution.

Nevertheless, these results suggest that the numerical calculation of the underlying admittance function is more feasible in terms of approximating an actual physical absorber.

5. FINAL COMMENTS AND CONCLUSIONS

The article presented a novel numerical method for estimating locally reactive impedance or admittance functions that ensure equivalent diffuse field absorption characteristics to an arbitrary target absorption function.

The absorption coefficient, being an energetic quantity, disregards the phase information of impedance and admittance characteristics. Additionally, diffuse absorption is averaged over all possible inclination angles. To address these challenges, the causality condition was applied, requiring all involved quantities to describe causal systems. Furthermore, locally reactive surfaces were assumed, where the angle dependence of the reflection coefficient and absorption factor is analytically known.

The proposed numerical method relies on the discrete Hilbert transform, enabling the formulation of the problem as a system of coupled nonlinear equations that can be solved using the Newton-Raphson method.

It was demonstrated that by selecting a suitable initial vector, both the surface impedance and admittance can be numerically calculated to ensure the desired diffuse absorption. Importantly, it was found that direct numerical solution with respect to the surface admittance provides a reasonable approximation of the underlying acoustic system.

However, as the system of equations still has an infinite number of solutions, further research is needed to investigate whether a priori assumptions about the underlying system can be incorporated into the method, such as choosing a model-dependent initial vector.

ACKNOWLEDGEMENTS

This work was supported by the OTKA PD-143129 grant, the János Bolyai Research Scholarship of the Hungarian Academy of Sciences, the ÚNKP-22-5-BME-318 New National Excellence Program of the Ministry for Innovation and Technology from the source of the National Research, Development and Innovation Fund and by ENTEL Engineering Research & Consulting Ltd., Hungary.

REFERENCES

1. ISO 354:2003. Standard, International Organization for Standardization, Geneva, CH, 2003.
2. H. Kuttruff. *Room Acoustics*. CRC Press, 2017.
3. B. Mondet, J. Brunskog, C. Jeong, and J. H. Rindel. From absorption to impedance: Enhancing boundary conditions in roomacoustic simulations. *Applied Acoustics*, 157, 2020.
4. J. H. Rindel. An impedance model for estimating the complex pressure reflection factor. In *In proceedings of Forum Acusticum 2011*, Aalborg, Denmark, 2011.
5. J. Gregory McDaniel. Applications of the causality condition to one-dimensional acoustic reflection problems. *J. Acoust. Soc. Am.*, 105(5):2710–2716, 1999.
6. A. N. Norris. Integral identities for reflection, transmission, and scattering coefficients. *J. Acoust. Soc. Am.*, 144(4):2019–2115, 2018.
7. S. L. Hahn. *The transforms and applications*. CRC and IEEE, 2000.
8. M. Shaker Sabbi and Willem Steenaart. Discrete hilbert transform filtering. *IEEE Transactions on Acoustics, Speech, and Signal Processing*, 25(5), 1977.
9. J. Gregory McDaniel and Cory L. Clarke. Interpretation and identification of minimum phase reflection coefficients. *J. Acoust. Soc. Am.*, 110(6):3003–3010, 2001.
10. E. Eisner. Minimum phase for continuous time and discrete time functions. *Geophys. Prospect.*, 32:533–541, 1984.
11. J. Allard and N. Atalla. *Propagation of Sound in Porous Media: Modelling Sound Absorbing Materials*. Wiley, 2009.
12. Y. Miki. Acoustical properties of porous materials-modification of delany-bazley models-. *J. Acoust. Soc. Jpn.*, 11(1), 1990.
13. J. F. Allard and Y. Champoux. New empirical equations for sound propagation in rigid frame fibrous materials. *J. Acoust. Soc. Am.*, 91(6), 1992.